

Spin coherence on the ferromagnetic spherical surface

A. R. Moura^{1,*}

¹*Departamento de Física, Universidade Federal de Viçosa, 36570-900, Viçosa, Minas Gerais, Brazil*

(Dated: February 18, 2022)

Spintronics on flat surfaces has been studied over the years, and the scenario is relatively well-known; however, there is a lack of information when we consider non-flat surfaces. In this paper, we are concerned about the spin dynamics of the ferromagnetic model on the spherical surface. We use the Schwinger bosonic formalism for describing the thermodynamics of spin operators in terms of spinon operators. Opposite to the flat two-dimensional model, which is disordered at finite temperature, the curvature of the spherical surface provides non-zero critical temperature for Schwinger boson condensation, which characterizes order at finite temperature even in the absence of external magnetic fields. The thermodynamics is then analyzed in the low-temperature regime. In addition, we consider the presence of both static and oscillating magnetic fields, the necessary condition for inducing the ferromagnetic resonance, and we show systematically that the studied model is well-described by $SU(2)$ coherent states, which provides the correct dynamics of the magnetization. The archived results can be applied for describing a diversity of experiments such as spin superfluidity, angular momentum injection by spin pumping and spin-transfer torque in non-conventional junctions, magnon dissipation, and magnetoelectronics on the spherical surface.

Keywords: Ferromagnetic Resonance; Spherical surface; Schwinger bosons

I. INTRODUCTION AND MOTIVATION

The continuous progress in spintronics has been motivated and supported by the potential realization of technologies based on spin degrees of freedom in favor of the electrical ones. Through a simple point-of-view, one of the principal purposes of spintronics is designing devices that work using spin currents as a substitute for the (electrical) charge currents (for an extensive review of spintronics, see Ref. [1] and [2]). Since spin currents occur in both normal metal and insulators, the applicability of spintronic devices is naturally higher than that one based on pure electronic transport. Spin currents can arise due to the Spin Hall Effect (SHE) [3, 4], the Spin Seebeck Effect (SSE) [5–7], or through Spin Pumping (SP) from ferromagnetic resonance (FMR) [8–12]. On the other hand, the detection of spin current is obtained by converting it into a charge current through the Inverse Spin Hall Effect (ISHE) [13–15] or the Inverse Rashba-Edelstein Effect (IRRE) [16]. One can use the Spin-Transfer Torque (STT) experiment for verifying spin current transport [17] as well.

In general, spintronic experiments involve flat surfaces and, therefore, there are no curvature effects in the thermodynamics of spin transport. However, the role of non-flat surfaces should be interesting for non-conventional geometric devices. For example, medical researches have widely used hollow magnetic nanoparticles as drug transporter [18–20]. At the same time, Hsu *et al.* showed the realization of the thin-film transistor on spherical surfaces [21, 22]. From the theoretical point-of-view, spherical surfaces have been used for studying the role of curved two-dimensional space in phase transition such

as Berezinskii-Kostertiz-Thouless (BKT) transition [23–25] and Bose-Einstein Condensation (BEC) [26, 27]. For the latter case, many experiments of ultra-cold atoms on spherical bubbles have been proposed [28, 29]; however, they require complex microgravity conditions to avoid the particles fall to the bottom of the trap [30–32]. Topological structures on curved manifold also were investigated in recent years. Kravchuck *et al.* studied out-of-surface vortices [33] and skyrmions [34] on spherical surfaces; curvature effects were shown to be associated with effective magnetic interactions that provide the spin field on curved manifolds [35, 36]; Sloika *et al.* determined the topological structure of the magnetization on spherical shells in terms of geometrical parameters. A review of topological spin field excitations on curved spaces can be found in Ref. [37].

In this article, we use the Schwinger bosonic formalism for investigating the magnetization thermodynamics of the ferromagnetic (FM) model on the spherical manifold. Despite the two-dimensional surface, the spherical model presents some three-dimensional characteristics. Indeed, opposite to the flat two-dimensional model, we find a finite phase transition temperature for all spin values. We choose the Schwinger Bosons Mean-Field Theory (SBMFT) because of its versatility for describing both ordered and disordered phases; however, in the present article, we are mainly interested in the low-temperature regime. Although SBMFT can be improved by taking into account Gaussian corrections in the mean-field parameters [38], the mean-field fluctuations have been mostly applied in frustrated antiferromagnetic (AFM) models [39–41], whilst the usual SBMFT seems to describe reasonably well the FM model, which is less susceptible to quantum fluctuations. In addition, we demonstrate that the Schwinger representation on the spherical surface does not present the pathological problem observed in flat space [42]. We show that the inter-

* antoniormoura@ufv.br

action with the oscillating magnetic field provides $SU(2)$ coherent states, which present similar points when compared with the $U(1)$ version. The magnetization and magnetic susceptibility are then determined using the $SU(2)$ coherent states of the Schwinger bosons, and the results are in agreement with the expected ones.

II. MODEL AND FORMALISM

We consider the ferromagnetic insulator described by the Hamiltonian $H(t) = H_0 + V(t)$, where the time-independent part is given by

$$H_0 = -J \sum_{\langle ij \rangle} \vec{S}_i \cdot \vec{S}_j - g\mu_B B^z \sum_i S_i^z, \quad (1)$$

in which the sum is taken over nearest-neighbor spins on the spherical surface, and $J > 0$ is the exchange coupling. The time-dependent term represents the interaction with the oscillating magnetic field, being expressed by

$$V(t) = -g\mu_B B^x(t) \sum_i S_i^x. \quad (2)$$

We are adopting both magnetic fields B^x and B^z as uniform fields based on the reduced dimensions of the samples in spintronic experiments. The interaction $V(t)$, which is treated according to the interaction picture, provides the coherent states necessary for the description of the magnetization precession.

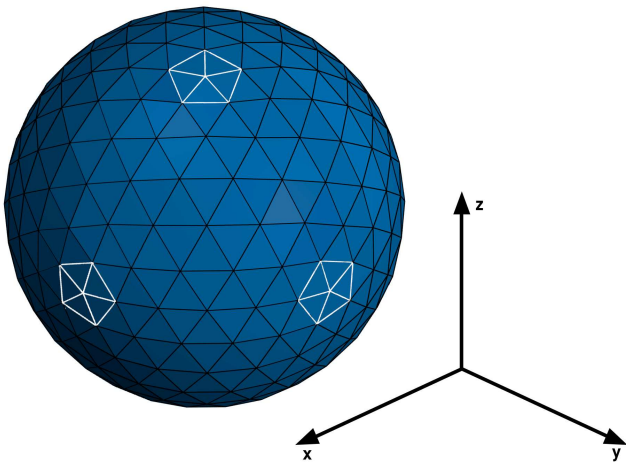


FIG. 1. Spherical tessellation of the icosahedron. The vertices of the polyhedron provide sites with five neighbors, while the other sites have six ones.

Opposite to the planar square lattice, in which each site always has four neighbors, it is impossible to build a regular discrete lattice on a spherical surface due to its topology. For a review of the lattice representations on the sphere, see Ref. [43]. For avoiding the singularities at the poles of the geographic coordinates grid, we

consider geometric tessellations based on the icosahedron [44]. Each side of the icosahedron is subdivided in a regular lattice and then, the sites are then projected onto the spherical surface. As one can see in fig. 1, most sites have six neighbors, while the vertices sites have five neighbors. The exact grid adopted is not so relevant since we use a continuous representation of the Hamiltonian (3); however, the number of neighbors z (coordination number) is important, and we will consider $z = 6$. Note that due to the triangular symmetry of the lattice, the antiferromagnetic model on the spherical surface will be frustrated, which requires special treatment for decoupling the quartic terms [45]. In addition, frustrated models are sensible to quantum fluctuations at low-temperatures and, in this case, the SBMFT need to be endowed with Gaussian corrections in the mean-field parameters [39–41]. Curiously, the spherical curvature implies changes in the winding number of topological solutions. The uniform solution, which presents the spin field align to a fixed direction, has winding number $Q = 1$, while $Q = 0$ for the lowest-energy skyrmion solution ($Q = 0$ and $Q \neq 0$ for the ground-state and skyrmion solutions, respectively, when we consider the flat two-dimensional space). In addition, the correct development of skyrmion-kind excitations requires the uniaxial anisotropy $(\vec{S} \cdot \vec{n})^2$, where \vec{n} is the outward normal vector, as pointed by Kravchuk *et al.* [34]. Here, since we do not interested in topological solutions, and due to the magnetic field B^z , which aligns the spin field along the z-axis, we do not consider the uniaxial anisotropy.

At low-temperature, spin operators are usually treated by using the Holstein-Primakoff (HP) bosonic representation[46]; however, HP bosons are inaccurate for representing disordered magnetic phases. The more appropriate representation is obtained through Schwinger bosons, which apply to both ordered and disordered phases [47, 48]. The spin operators are then replaced by two kinds of bosonic operators and written as $S_i^+ = a_i^\dagger b_i$, $S_i^- = b_i^\dagger a_i$, and $S_i^z = (a_i^\dagger a_i - b_i^\dagger b_i)/2$, where a_i^\dagger (b_i^\dagger) creates a spinon with spin 1/2 (-1/2) in the site i . For ensuring the commutation relation $[S_i^a, S_j^b] = i\delta_{ij}\epsilon_{abc}S_i^c$, it is necessary to fix the number of bosons on each site through the local constraint $a_i^\dagger a_i + b_i^\dagger b_i = 2S$. Note that the spin operators are invariant under the $U(1)$ gauge transformation $a_i \rightarrow e^{i\psi} a_i$ and $b_i \rightarrow e^{i\psi} b_i$, where ψ is a global phase. Therefore, the Hamiltonian H_0 is written as

$$H_0 = -\frac{J}{2} \sum_{\langle ij \rangle} (: \mathcal{F}_{ij}^\dagger \mathcal{F}_{ij} : - 2S^2) + \sum_i \lambda_i (\mathcal{F}_{ii} - 2S) - \frac{g\mu_B B^z}{2} \sum_i (a_i^\dagger a_i - b_i^\dagger b_i) \quad (3)$$

in which we defined the bond operator $\mathcal{F}_{ij} = a_i^\dagger a_j + b_i^\dagger b_j$ and $: :$ represents the normal ordering operator. The constraint is implemented by a local Lagrange multiplier

λ_i , and the quartic order term is decoupled by introducing the auxiliary field $F_{ij} = \langle \mathcal{F}_{ij} \rangle$ through the Hubbard-Stratonovich transform $\mathcal{F}_{ij}^\dagger \mathcal{F}_{ij} \rightarrow F_{ij}(\mathcal{F}_{ij}^\dagger + \mathcal{F}_{ij}) - F_{ij}^2$. As usual, we adopt the mean-field theory and F_{ij} is replaced by the uniform field F . We also approximate the Lagrange multiplier by a uniform parameter λ that implies boson conservation only on average. In general, SBMFT is successful to describe the thermodynamic of magnetic models but is also known that SBMFT gives the incorrect local spin-spin correlation due to the missing of a multiplicative 2/3 factor [47, 49]. The problems with the mean-field theory are more evident when quantum fluctuations are more relevant, as occurs in frustrated AFM models, for example. To correct this inconvenience, Gaussian corrections can be implemented in the SBMFT [38]; however, since we are considering the FM model in the coherent state, quantum fluctuations have a minor effect (opposite to frustrated AFM models) and the mean-field theory is supposed to provide reasonable results.

The diagonalization of Eq. (3) involves the continuous limit, which also provides an easy method for including the curvature effect. In the long-wavelength limit, we adopt the second-order expansion $a_j \approx a_i + \varepsilon^k \partial_k a_i + (\varepsilon^k \varepsilon^l / 2) \partial_k \partial_l a_i$, where ε^k are infinitesimal displacements along the polar or azimuth directions, and the sums in k and l are implicit. The expansion results in $\sum_{\langle ij \rangle} a_i^\dagger a_j \approx \int d\Omega z \sigma [a^\dagger a + (\varepsilon^2/4) a^\dagger \nabla^2 a]$, where $d\Omega = \sin \theta d\theta d\varphi$ with $0 \leq \theta \leq \pi$ and $0 \leq \varphi < 2\pi$ being the polar and azimuth angles, respectively. The (angular) density of states on the spherical surface is defined as $\sigma = \mathcal{N}/4\pi$, and we choose ε in order to obtain $R^2 = \sigma \varepsilon^2$, where R is the sphere radius. We write the continuous $a(\theta, \varphi)$ operator as the following spherical harmonic expansion

$$a(\theta, \varphi) = \frac{1}{\sqrt{\sigma}} \sum_L a_L Y_L(\theta, \varphi), \quad (4)$$

where L stands for a compact notation of lm , with l integer and $m = -l, -l+1, \dots, l-1, l$. The same procedure is applied for the b operator. The σ factor is included for ensuring the same number of bosonic modes on both bases, *i.e.* $\sum_i a_i^\dagger a_i = \sum_L a_L^\dagger a_L$. In addition, we introduce a superior limit l_{\max} for the l sum. This restriction is expected since in the continuous representation we have considered smooth operators in the expansion of a_j , and spherical harmonics with fast oscillations ($l > l_{\max}$) have negligible contributions. Therefore, assuming the lattice parameter as a space cutoff, and adopting one-to-one correspondence between the representations, we obtain $\mathcal{N} = \sum_i = \sum_L = (l_{\max} + 1)^2$. Using the properties of the spherical harmonics, it is straightforward to obtain

$$H_0 = E_0 + \sum_L \left(\epsilon_L^{(a)} a_L^\dagger a_L + \epsilon_L^{(b)} b_L^\dagger b_L \right), \quad (5)$$

where $E_0/\mathcal{N} = zJF^2/2 - 2S(zJF - \mu)$ is a constant energy, $\epsilon_L^{(a)} = \epsilon_L - \mu - g\mu_B B^z/2$, $\epsilon_L^{(b)} = \epsilon_L - \mu + g\mu_B B^z/2$,

$\mu = zJF - \lambda$ plays the role of a chemical potential (we can also define $-\mu$ as the gap energy), and $\epsilon_L = zJFl(l+1)/4\sigma$ is the $(2l+1)$ -fold degenerate energy mode. In Appendix (B), we developed the Linear Spin-Wave (LSW) theory using the HP bosonic formalism. At very low temperatures, the results obtained from both formalism are identical.

A. Generation of the coherent states

For obtaining the magnetization precession, it is necessary to apply an oscillating magnetic field perpendicular to the static field B^z . The relation between the coherent states and the oscillating field is deduced as follows. Through the spherical Schwinger bosons, we write $\sum_i S_i^x = (J^+ + J^-)/2$, where we define the many-site operators $J^+ = J^x + iJ^y = \sum_L a_L^\dagger b_L (= \sum_i a_i^\dagger b_i)$ and $J^- = (J^+)^{\dagger}$, which follow the Lie algebra

$$[J^a, J^b] = i\epsilon_{abc} J^c, \quad (6)$$

in which the structure constants are given by the Levi-Civita symbol ϵ_{abc} . Therefore, the Hamiltonian H is expressed in terms of the generators of the group $SU(2)$. We choose a basis in terms of the eigenstates of the operator $J^z = \sum_L (a_L^\dagger a_L - b_L^\dagger b_L)/2$, namely $|jj_z\rangle$, with j integer or half-integer and $j_z = -j, -j+1, \dots, j-1, j$. The Casimir operator $J^2 = (J^z)^2 + (J^+ J^- + J^- J^+)/2$ satisfies $[J^z, J^2] = 0$ as well as the eigenvalue equation $J^2 |jj_z\rangle = \hbar j(j+1) |jj_z\rangle$, as observed for standard angular momentum operators. In our case, J represents the angular momentum sum of \mathcal{N} sites with spin S on the spherical surface, and the Hilbert space is spanned as the direct sum of irreducible representations according to j . Since \mathcal{N} is odd, the minimum $j_{\min} = S$ is obtained when $\mathcal{N} - 1$ sites are paired with opposite spin, and the maximum $j_{\max} = \mathcal{N}S$ occurs when the \mathcal{N} sites are unpaired. Here and henceforth, we will consider a fixed j and define the lowest-weight (extremal state) $|j-j\rangle$ as $|\Psi_0\rangle$.

Any element $g \in SU(2)$ can be expressed as

$$g = D(\theta, \varphi) h, \quad (7)$$

where $h = \exp(i\alpha J^z)$ is an element of the group $U(1)$, with α being a real parameter, and $D(\theta, \varphi)$ is the coset representative of $SU(2)/U(1)$, *i.e.* the two-dimensional sphere S^2 . One can show that $D(\theta, \varphi) = \exp(i\theta \vec{m} \cdot \vec{J})$, with $\vec{m} = (\sin \varphi, -\cos \varphi, 0)$ and, therefore, $D(\theta, \varphi)$ provides (except for a multiplicative constant chosen to be unity) the coherent state $|\vec{n}\rangle$ given by [50, 51]

$$|\vec{n}\rangle = D(\theta, \varphi) |\Psi_0\rangle. \quad (8)$$

Physically, the state $|\vec{n}\rangle$ represents the classical vector $\vec{n} = (\sin \theta \cos \varphi, \sin \theta \sin \varphi, \cos \theta)$, and $D(\theta, \varphi)$ is the so-called generalized displacement operator. For our present purpose, it is more convenient to express the operator D as

$$D(\zeta) = e^{\zeta J^+ - \bar{\zeta} J^-}, \quad (9)$$

in which $\zeta = -(\theta/2)\exp(-i\varphi)$ is a complex parameter. Note that all spins are described by the same angles θ and φ , which is characteristic of magnetization precession. In addition, the above expression makes clear the similarity between $D(\zeta)$ and the displacement operator of the $U(1)$ coherent state theory [52], which justifies the chosen name.

Returning to the Hamiltonian H , we write the time-dependent average of an operator $A(t)$ in the Interaction picture

$$\langle A(t) \rangle = \langle \Psi_0 | U^\dagger(t, -\infty) \hat{A}(t) U(t, -\infty) | \Psi_0 \rangle, \quad (10)$$

with the caret denoting time evolution according H_0 and

$$U(t, -\infty) = T_t \exp\left(-\frac{i}{\hbar} \int_{-\infty}^t \hat{V}(t') dt'\right), \quad (11)$$

where T_t is the time-ordering operator. Here, we consider an adiabatic process from the dim past ($t \rightarrow \infty$), for which the interaction is off and the ground-state is $|\Psi_0\rangle$, to the present time with full Hamiltonian $H(t) = H_0 + V(t)$. It is a straightforward procedure to show that the argument of the exponential of U is given by $\zeta(t)J^+ - \bar{\zeta}(t)J^-$, where

$$\zeta(t) = \frac{ig\mu_B}{2\hbar} \int_{-\infty}^t B^x(t') \exp\left[\frac{i}{\hbar}(\epsilon_0^{(a)} - \epsilon_0^{(b)})t'\right]. \quad (12)$$

Despite an irrelevant phase factor, we can show that

$$U(t, -\infty)|\Psi_0\rangle = D(\zeta)|\Psi_0\rangle = |\zeta\rangle, \quad (13)$$

and the oscillating magnetic field generates the $SU(2)$ coherent state $|\zeta\rangle$. As usual in experiments, we adopt a monochromatic magnetic field with frequency ω_{rf} , for which we obtain

$$\zeta(t) = \frac{\gamma B^x}{2(\gamma B^z - \omega_{\text{rf}} - i\eta)} e^{i(\gamma B^z - \omega_{\text{rf}})t}, \quad (14)$$

where $\gamma = g\mu_B/\hbar$ is the gyromagnetic ratio, and the factor η is added for ensuring the convergence in the limit $t \rightarrow -\infty$.

III. THERMODYNAMICS AT LOW-TEMPERATURE

Since the Hamiltonian H_0 is described by coherent states, we can write the partition function as $Z_0 = \int D[\bar{a}, a] D[\bar{b}, b] \exp[-\mathcal{S}/\hbar]$, where the integration measures represent the integration on each point on the continuous spherical surface (for more details, see Appendix A). Note that, since we have adopted the mean-field replacement for F and λ , the partition function does not involve path integration over F and λ . In the spherical harmonic space, the action is given by

$$\mathcal{S} = \beta\hbar E_0 + \frac{\beta\hbar}{2} \sum_{i\omega_p} \sum_L \left[\bar{a}_L(-i\hbar\omega_p + \epsilon_L^{(a)}) a_L + \bar{b}_L(-i\hbar\omega_p + \epsilon_L^{(b)}) b_L + \text{h.c.} \right], \quad (15)$$

with the Matsubara frequencies $\omega_p = 2\pi p/\beta\hbar$, $p \in \mathbb{Z}$. Here, for convenience, we use the same notation a_L and b_L for representing the fields associated with the correspondent operators a_L and b_L , respectively. The meaning of a_L and b_L should be clear from the context but, if necessary, a comment will be inserted. After integrating out the fields, we obtain the mean-field free energy

$$F_{\text{MF}} = E_0 + \frac{1}{2\beta} \sum_{i\omega_p} \sum_L \ln(\beta M) \quad (16)$$

where $M = \epsilon_L^{(a)}(I + \sigma_z) \otimes I/2 + \epsilon_L^{(b)}(I - \sigma_z) \otimes I/2 - i\hbar\omega_p I \otimes \sigma_z$. Provided that $F_{\text{MF}} = E_0$ in the limit $T \rightarrow 0$, the Matsubara frequency sum results in

$$F_{\text{MF}} = E_0 + \frac{1}{\beta} \sum_L \ln \left[(1 - e^{-\beta\epsilon_L^{(a)}})(1 - e^{-\beta\epsilon_L^{(b)}}) \right]. \quad (17)$$

In the presence of the magnetic field B^z , a broken symmetry takes place at low-temperatures, as expected. The more interesting case occurs in the limit of vanishing magnetic field B^z . For a flat two-dimensional model (with only short-range interactions and continuous symmetry) free of magnetic fields, there is no ordering at finite temperature; however, the situation is different for the spherical manifold. Indeed, the impossibility of magnetic ordering at finite temperature comes from the Mermin-Wagner theorem, which requires thermodynamic limit for yielding low-energy Goldstone modes. Insofar as the spherical surface is compact, the Mermin-Wagner theorem is not applicable and would be possible to observe spontaneously broken symmetry at finite temperatures.

In the Schwinger bosonic formalism, an ordered state is related to the BEC of the spinon modes [48]. Below a critical temperature T_c , the chemical potential vanishes, and the bosons condensate in the minimal energy state $\epsilon_{l=0}$, while for $T > T_c$, $\mu < 0$. The connection between the magnon-picture and the spinon-picture is given as following. The up-spin spinon band represents the ordered ground state, while the down-spin spinon is associated with the spin excitation. Therefore, a magnon is described by an up spinon that suffers a transition to a down-spin spinon. Note that creation/annihilation spinon processes only happen in pairs and free spinons are not observed in FM models. For taking into account the BEC, we separate the $l = 0$ term from the sum, which is indicated by a prime, and write the free energy per site as

$$\frac{F_{\text{MF}}}{\mathcal{N}} = f_{\text{MF}} = \frac{\xi^2}{2zJ} - 2S\xi[1 + (1 - \rho)\Delta] + \frac{2}{\beta\mathcal{N}} \sum'_L \ln \left[1 - e^{-\frac{1}{t}(\frac{L+1}{4\sigma} + \Delta)} \right], \quad (18)$$

where $\xi = zJF$ is the energy scale, $\Delta = -\mu/\xi$ is the dimensionless gap energy, $t = k_B T/\xi$ is the reduced temperature, and $\rho = \mathcal{N}_0/\mathcal{N}$ measures the condensation level. At low-temperatures, the exponential decreases fast enough, and we can evaluate the sum replacing it by an integral. Using the Mercator series $\ln(1 - x) = -\sum_{k=1}^{\infty} x^k/k$, we obtain

$$f_{\text{MF}} = \frac{\xi^2}{2zJ} - 2S\xi[1 + (1 - \rho)\Delta] - \frac{2\xi t^2}{\pi} \text{Li}_2(ge^{-1/2t\sigma}), \quad (19)$$

where Li_s is the polylogarithmic function of order s and $g = \exp(-\Delta/t)$ is the fugacity. The parameters ξ and Δ are then determined by the extremum conditions $\partial f_{\text{MF}}/\partial \Delta = 0$ and $\partial f_{\text{MF}}/\partial \xi = 0$, which provide

$$\rho = 1 - \frac{t}{\pi S} \text{Li}_1(ge^{-1/2t\sigma}), \quad (20)$$

and

$$\frac{\xi}{zJ} = 2S - \frac{2t^2}{\pi} \text{Li}_2(ge^{-1/2t\sigma}) \quad (21)$$

respectively. Observe that $\Delta = 0$ and $0 < \rho \leq 1$ below the critical temperature, while $\Delta > 0$ and $\rho = 0$ for $T > T_c$. The reduced critical temperature t_c is then obtained making $\rho = 0$ and $\Delta = 0$ in Eq. (20), which results in the self-consistent equation

$$t_c = \frac{\pi S}{\text{Li}_1(e^{-1/2t_c\sigma})} \quad (22)$$

Since both ρ and ξ parameters depend only on the reduced temperature, it is easy to solve the equations. One can also obtain the above equations without performing the continuum approximation. Figure 2 shows the results for the condensation by using the two approaches, directly from the sum and through the polylogarithmic equation. As one can see, both curves are close at low-temperatures. For $S = 1$ and $\mathcal{N} = 10^6$, we obtain $t_c = 0.25$ evaluating the sum over L , and $t_c = 0.26$ when we use Eq. (22). The chemical potential is also determined using both methods and the results are shown in fig. 3. Again, the difference between the polylogarithmic and the result obtained from the sum is small at low-temperatures.

The reduced critical temperature is shown in fig. 4. The critical temperature is a decreasing function of increasing density of states, and t_c tends to zero in the limit of $\sigma \rightarrow \infty$. Indeed, when σ is very large, the distance between nearest-neighbors on the surface is small and the curvature effect is negligible. Locally, the short-range interaction resembles the flat-space interaction, and we

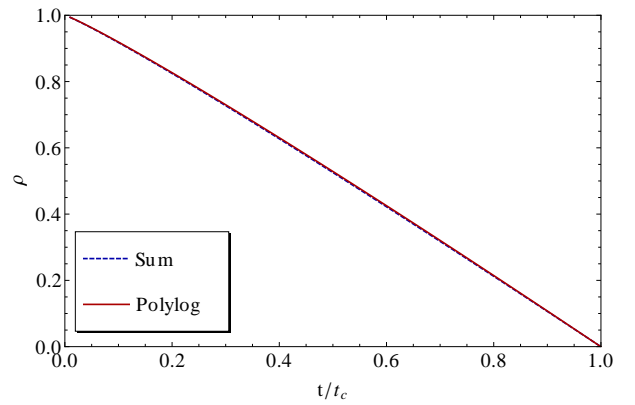


FIG. 2. The condensation ρ as a function of the reduced temperature. The results obtained by using the sum on l and m and from the continuum (polylogarithmic) approximation are close. Here, we consider $\mathcal{N} = 10^6$, $S = 1$, $t_c = 0.26$ (Polylog result) and $t_c = 0.25$ (Sum result).

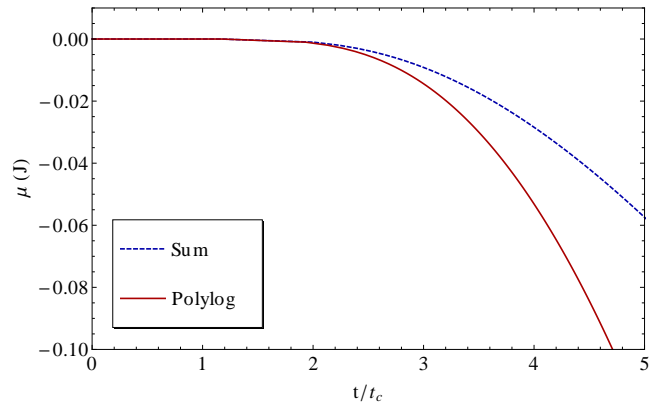


FIG. 3. The chemical potential determined through the polylogarithmic approximation and by the sum over L . Here, we adopt $\mathcal{N} = 10^6$, $S = 1$ and $t_c = 0.26$.

recovery the flat two-dimensional result, for which the critical temperature $T_c = 0$. In addition, there is no critical spin and the transition temperature is finite for any spin value, including the classical limit $S \gg 1$. Here, for sake of simplicity, we consider $S = 1$.

The polylogarithmic approximation is very reasonable in the ordered state; however, when $t > t_c$ the approximated equations are not accurate, and any result should be determined by using the equations written in terms of the sum over L . The problem occurs due to the slow decreasing of the exponential in Eq. (18) when $k_B T > zJF$, which precludes the series expansion of the logarithmic function. To verify the spurious result of the approximation at high temperature, we analyze the relation between the physical and reduced temperature given by $T(t) = t\xi(t)$ and shown in fig. 5. The function $T(t)$ obtained by the approximation shows a maximum at $t_{\text{max}} \approx 3.1t_c$, and for $t > t_{\text{max}}$, T decreases with increasing t , for which we obtain a non-physical result. Indeed,

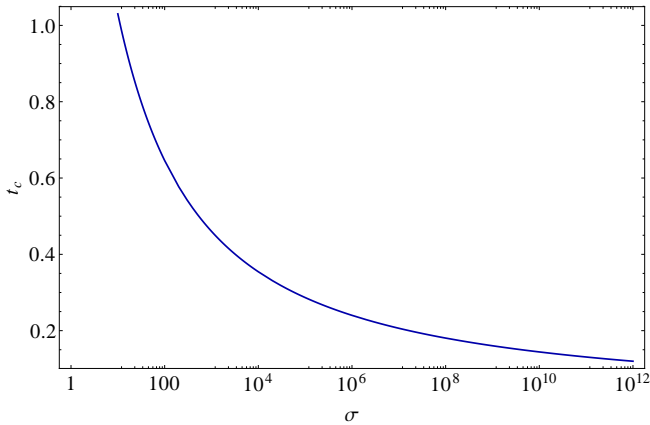


FIG. 4. The reduced critical temperature dependence on the density of sites. Locally, the limit $\sigma \rightarrow \infty$ reflects the flat space, which provides $t_c \rightarrow 0$.

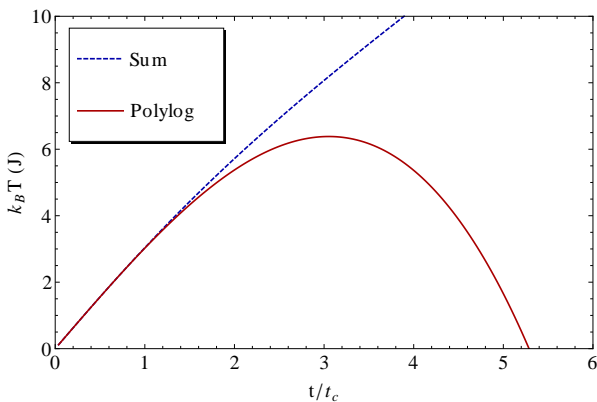


FIG. 5. The relation between the physical T and the reduced t temperatures. For $t > t_c$, the approximated polylogarithmic equations present spurious results.

because of the decreasing behavior of $T(t)$, $F(T)$ shows an increasing function of increasing T , as shown in fig. 6, where the dotted branch represents the spurious result obtained through the approximation for $t > t_c$. The correct behavior, which shows a decreasing F for increasing T , is obtained when we use the equations for ξ and ρ written using the sum over L . The spurious branch also appears in the three-dimensional ferromagnetic model, as pointed in Ref. ([42]) (in this case, the Schwinger formalism presents serious problems for describing spin models with $S \gtrsim 0.15$). Since we are interested in the ordered state ($t < t_c$), we keep the polylogarithmic approximation.

It is important to note that the limit of high temperatures ($t \gg t_c$) can not be described by the equations developed above. Provided that we consider only long-wavelength spin-wave in the continuous description of the Hamiltonian, high-energy excitations are not covered by the present model. For including the high-energy spec-

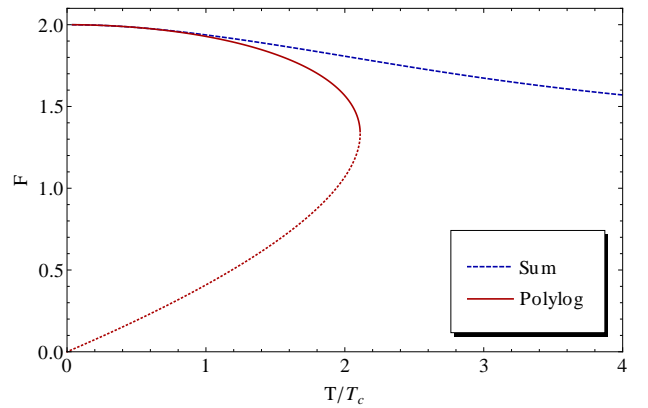


FIG. 6. The average ferromagnetic bond F as function of T . For $t > t_c$, we obtain the dotted branch, which is non-physical. Here, $T_c = t_c \xi(t_c)$, with $t_c = 0.26$.

trum, one should write $\sum_{\langle ij \rangle} a_i^\dagger a_j = \sum_L \gamma_L a_L^\dagger a_L$, where the structure factor is given by

$$\gamma_L = \sum_{\eta_\theta, \eta_\varphi} \int d\Omega \bar{Y}_L(\theta, \varphi) Y_L(\theta + \eta_\theta, \varphi + \eta_\varphi), \quad (23)$$

and $\eta_{(\theta, \varphi)}$ are the angular nearest-neighbor positions. Expanding the neighbor sites around (θ, φ) , we obtain $\gamma_L \approx z - z l(l+1)/4\sigma$, which recovers the Hamiltonian (5). Since we are interested in the low-energy limit, it is not necessary consider the full structure factor.

When the magnetic field B^z is included, the equations are obtained following the same steps, and the only difference occurs in the condensation. In this case, since the b modes acquired a gap due to the Zeeman energy, only the a bosons condensate in the $l = 0$ state. The critical temperature, for example, is then given by

$$t_c = \frac{2\pi S}{\text{Li}_1(e^{-1/2t_c\sigma}) + \text{Li}_1(e^{-(1/2\sigma + \hbar\gamma B^z)/t_c})}, \quad (24)$$

which recovers Eq. (22) when $B^z = 0$.

IV. MAGNETIZATION DYNAMICS

To determine the dynamics of the spin $\vec{S}_i(t)$, and so the surface magnetization defined by $\vec{M} = (\gamma\hbar/\mathcal{N}\varepsilon^2) \sum_i \langle \vec{S}_i \rangle$, let us define the coherent state $|\zeta_i\rangle$. Using the Baker-Campbell-Hausdorff (BCH) formula, the generalized displacement operator for the i site is expressed as

$$D(\zeta_i) = e^{\kappa_i J_i^+} e^{\ln(1+|\kappa_i|^2) J_i^z} e^{-\kappa_i J_i^-}, \quad (25)$$

with $J_i^+ = a_i^\dagger b_i$, $J_i^z = (a_i^\dagger a_i - b_i^\dagger b_i)/2$, and $\kappa_i = \exp(-i\varphi_i) \tan(\theta_i/2)$. When applied on the extremum state $|\psi_0\rangle$, for which $S^z |\psi_0\rangle = -S |\psi_0\rangle$, the displacement operator provides

$$D(\zeta_i) |\psi_0\rangle = \frac{1}{(1+|\kappa_i|^2)^S} e^{\kappa_i J_i^+} |\psi_0\rangle. \quad (26)$$

Since $|\psi_0\rangle$ represents the state with $n_a = 0$ and $n_b = 2S$, the operator J_i^+ can be applied a maximum of $2S$ times, and the k -th operation results in $(J_i^+)^k|\psi_0\rangle = [(2S)!k!/(2S-k)!]^{1/2}|n_a = S, n_b = 2S - k\rangle$. Therefore, we obtain

$$|\zeta_i\rangle_{2S} = D(\zeta_i)|\psi_0\rangle = \sqrt{(2S)!} \sum_{n_a, n_b} \frac{u_i^{n_a} v_i^{n_b}}{\sqrt{n_a! n_b!}} |n_a, n_b\rangle, \quad (27)$$

where the implicit local constraint $n_a + n_b = 2S$ is assumed in the sum, which is indicated by the subscript $2S$ in $|\zeta_i\rangle$, and we define the local parameters

$$u_i = \cos\left(\frac{\theta_i}{2}\right), \quad (28)$$

and

$$v_i = \sin\left(\frac{\theta_i}{2}\right) e^{-i\varphi_i}. \quad (29)$$

Due to the finite sum, the $SU(2)$ coherent states are not eigenstates of the annihilation operators, as seen in the $U(1)$ representation; however, a straightforward procedure shows that

$$a_i|\zeta_i\rangle_{2S} = \sqrt{2S}u_i|\zeta_i\rangle_{2S-1}, \quad (30)$$

and

$$b_i|\zeta_i\rangle_{2S} = \sqrt{2S}v_i|\zeta_i\rangle_{2S-1}. \quad (31)$$

Therefore, $|\zeta_i\rangle$ plays a similar rule to that present in the $U(1)$ coherent state formalism and using the above equations, it is easy to show that the $SU(2)$ coherent states give the average $\langle a_i^\dagger a_i + b_i^\dagger b_i \rangle = 2S$.

Considering $|\zeta| < \pi/2$, equation (14) gives the global angles $\theta = \gamma B^x / (\gamma B^z - \omega_{\text{rf}} - i\eta)$ [for $|\zeta| > \pi/2$, we define the polar angle by $4\theta = \gamma B^x / (\gamma B^z - \omega_{\text{rf}} - i\eta) \bmod 2\pi$] and $\varphi = (\omega_{\text{rf}} - \gamma B^z)t$. The z-component of the magnetization is time-independent and given by $M^z = \gamma\hbar\langle\cos\theta\rangle \approx \gamma\hbar$ for small polar angles, as expected when \vec{M} involves according to precession dynamics. For analyzing the perpendicular magnetization component, we define the complex field $M^\perp = M^x + iM^y = (\gamma\hbar/\mathcal{N}) \sum_i a_i^\dagger b_i$, which yields the uniform magnetization $M^\perp(t) = \gamma\hbar S e^{-i\gamma B^z t} \langle \sin\theta e^{-i\varphi} \rangle$, and for small θ , we get

$$M^\perp(t) = \frac{M_s \gamma B^\perp(t)}{\gamma B^z - \omega_{\text{rf}} - i\eta}, \quad (32)$$

where $B^\perp(t) = \mu_0[H^\perp(t) + M^\perp(t)] = B^x e^{-i\omega_{\text{rf}} t}$ is a monochromatic field, and $M_s = \gamma\hbar S/\varepsilon^2$ is the saturation magnetization on the spherical surface. In the spherical harmonic-frequency space, the magnetization is written as $M_L^\perp(\omega) = \sum_{L'} \chi_{LL'}(\omega) H_{L'}^\perp(\omega)$. Note that for uniform monochromatic field and magnetization, the only accessible mode of the susceptibility is $\chi_{00}(\omega_{\text{rf}})$. Then, using

Eq. (32), we obtain the long-wavelength magnetic susceptibility $\chi_{00} = \chi' + i\chi''$, where the uniform real and complex parts are given by

$$\chi' = \frac{\omega_M(\omega_0 - \omega_{\text{rf}})}{(\omega_0 - \omega_{\text{rf}})^2 + \eta^2} \quad (33)$$

and

$$\chi'' = \frac{\omega_M \eta}{(\omega_0 - \omega_{\text{rf}})^2 + \eta^2}, \quad (34)$$

respectively. In above equations, $\omega_0 = \gamma\mu_0 H^z$ is the frequency of the lowest-energy magnons, and η is related to the Gilbert damping. As one can see, the magnetic response is maximum when magnetic fields satisfy $\gamma\mu_0 H^z = \omega_{\text{rf}}$, the resonating condition. Typical experiments involve resonating frequencies of the order of GHz and H^z of the order of 10^{-1} T [9, 12, 53]. Through the definition of M_L^\perp and H_L^\perp , one can also determine the real susceptibilities $\chi^{xx} = \chi^{yy} = \chi'$, and $\chi^{yx} = -\chi^{xy} = \chi''$. Note that the magnetization precession presents a response in both field directions H^x and H^y . The delay effect is caused by the spin relaxation and, in the opposite case, when $\eta = 0$, the magnetization instantly responds to the field application. Hence, in the driven magnetization precession, the magnetic susceptibility on the spherical surface presents the same behavior observed in flat models [54]. Indeed, provided that we are dealing with uniform fields, it is expected only the $q = 0$ (for flat geometry) or $L = 0$ (for spherical geometry) susceptibility term. The uniform nature is then similar in both spaces. On the other hand, if the gradient of the magnetic field is included, the geometry influence is evidenced by the non-uniform terms in the expansion of χ .

V. SUMMARY AND CONCLUSIONS

In this article, we investigated the thermodynamics of the ferromagnetic model on the spherical surface. Similar problems involving flat surfaces have been studied in recent years; however there is a lack of information about spintronics of ferromagnetic models on curved spaces, and the present work was developed for clarifying some points of the theme.

The Hamiltonian was described by using the SBMFT, which represents the spin operators in terms of two kinds of bosons, a and b . Provided that we are dealing with the coherent state of an FM model, we expected a minor influence of fluctuations in the mean-field parameters, and Gaussian corrections were not included in this work. Opposite to the flat surfaces, we found a finite critical temperature T_c that separates the ordered phase from the disordered one. The critical temperature depends on the density of sites σ , and we recovery the result $T_c = 0$ in the limit $\sigma \rightarrow \infty$, which is the local representation of the two-dimensional flat surface. We showed that, at the low-temperature limit, the developed equations give

trustworthy results. In addition, we analyzed the magnetization dynamics in the presence of two orthogonal magnetic fields; the static field B^z that aligns the spin field and the oscillating field $B^x(t)$ responsible for the precession motion. We demonstrated systematically that in the presence of the cited magnetic fields, the model is described by $SU(2)$ coherent states, which are suitable for evaluating all thermodynamic properties. The magnetization behavior and the magnetic susceptibility were evaluated through the coherent states, and the results are in agreement with the expected ones obtained from the Linear Spin-Wave theory developed in Appendix (B). Indeed, we found that the more efficient magnetization precession occurs at the resonant condition $\omega_{\text{rf}} = g\mu_0 H^z$, for instance.

In summary, we showed that the description of ferromagnetism and spintronics on the spherical surface can be developed through the $SU(2)$ coherent states. Here, we applied the formalism for describing the magnetization precession; however, other spin experiments on curved space such as spin superfluidity, spin current injection, spin-transfer torque, and spin-wave dissipation processes, can also be explained by the developed method. In addition, magnetic models on the spherical surface could be used for testing general curvature effects in favor of the complicated experiments on curved space, like the microgravity experiments for verifying BEC on spherical manifold, for example.

Appendix A: Path integral for $SU(2)$ coherent states

We can use the $SU(2)$ coherent states for evaluating the partition function through the path integral formalism. Let us adopt the following Hamiltonian

$$H_0 = \sum_{\langle ij \rangle} (\epsilon_{ij}^{(a)} a_i^\dagger a_j + \epsilon_{ij}^{(b)} b_i^\dagger b_j), \quad (\text{A1})$$

written in terms of the Schwinger bosons a and b .

Following the standard path integral procedures, we divide the time interval in N small $\Delta\tau$ steps, with $\tau_0 = 0$ and $\tau_N = \beta\hbar$, which provide the partition function

$$Z_0 = \sum_{\zeta} \langle \zeta(\tau_N) | \prod_{p=1}^N e^{-\hat{H}_0(\tau_p)\Delta\tau} | \zeta(\tau_0) \rangle, \quad (\text{A2})$$

with the periodic condition $|\zeta(\tau_N)\rangle = |\zeta(\tau_0)\rangle = \prod_i |\zeta_i\rangle$ (here, the $2S$ subscript was omitted for simplifying the notation). Inserting the identity $I = \int d\zeta |\zeta\rangle \langle \zeta|$ between the intervals, we obtain

$$\langle \zeta(\tau_p) | e^{-\hat{H}_0\Delta\tau} | \zeta(\tau_p - \Delta\tau) \rangle \simeq 1 - \langle \zeta(\tau_p) | \dot{\zeta}(\tau_p) \rangle \Delta\tau - H_0(\tau_p), \quad (\text{A3})$$

where $H_0(\tau_p) = \langle \zeta(\tau_p) | \hat{H}_0 | \zeta(\tau_p) \rangle$ is an ordinary real function obtained through the replacement of the operators a_i and b_i by the respective fields $a_i = \sqrt{2S}u_i$ and

$b_i = \sqrt{2S}v_i$ [see Eq.(30) and (31)]. Note that, although $|\zeta\rangle$ is not an annihilation eigenstate, as occurs in the $U(1)$ coherent state, yet is possible for evaluating the average $\langle \exp(-\hat{H}_0\Delta\tau) \rangle$. The second term in the above equation is the Berry phase $\Omega_B = -iS \sum_i [\dot{\varphi}_i(1 - \cos\theta_i)]$. It is a straightforward evaluation for showing $\sum_i (\bar{a}_i \dot{a}_i + \bar{b}_i \dot{b}_i) = \Omega_B$. Therefore, the partition function is written as the path integral $Z_0 = \int D[\bar{a}, a] D[\bar{b}, b] \exp(-S/\hbar)$, where the action is given by

$$S = \int_0^{\beta\hbar} d\tau \left[\hbar \sum_i (\bar{a}_i \partial_\tau a_i + \bar{b}_i \partial_\tau b_i) + H_0(\tau) \right]. \quad (\text{A4})$$

Appendix B: Linear Spin-Wave Approximation

In order to compare the results of the $SU(2)$ coherent states obtained from the SBMFT, we develop the Linear Spin-Wave theory through the Holstein-Primakoff formalism[46]. Applying the gauge fixing condition $a = a^\dagger$ in the Schwinger formalism, one can obtain the HP bosonic representation of the spin operators: $S_i^+ = \sqrt{2S - b_i^\dagger b_i} b_i$, $S_i^- = b_i^\dagger \sqrt{2S - b_i^\dagger b_i}$ and $S_i^z = S - b_i^\dagger b_i$ [55]. At low temperatures, the LSW approximation is expected to provide reasonable results, and we adopt the approximation $S_i^+ \approx \sqrt{2S} b_i$ and $S_i^- \approx \sqrt{2S} b_i^\dagger$. Therefore, the quadratic Hamiltonian, given by Eq. (1), is written as

$$H_0 = JS \sum_{\langle ij \rangle} b_i^\dagger (b_i - b_j) - \gamma \hbar B^z \sum_i (S - b_i^\dagger b_i), \quad (\text{B1})$$

where $\gamma = g\mu_B/\hbar$ is the gyromagnetic ratio. After expanding b_j around b_i , the continuum limit is taken into account, which provides the Hamiltonian

$$H_0 = \int d\Omega b^\dagger \left(-\frac{zJSR^2\nabla^2}{4} + \gamma \hbar \sigma B^z \right) b. \quad (\text{B2})$$

The spherical harmonic expansion

$$b(\theta, \varphi) = \frac{1}{\sqrt{\sigma}} \sum_L b_L Y_L(\theta, \varphi), \quad (\text{B3})$$

then results in $H_0 = \sum_L (\epsilon_L + \gamma \hbar B^z) b_L^\dagger b_L$, where $\epsilon_L = zJS l(l+1)/4\sigma$ (L is the compact representation of $m = -l, -l+1, \dots, l-1, l$ and $l = 0, 1, 2, \dots$). This is the same spectrum energy obtained from the Schwinger bosonic formalism, see Eq.(5), in the very low-temperature limit. In this limit, we can approximate the mean-field parameter as $F \approx 2S$ and adopted the chemical potential $\mu = -\gamma \hbar B^z/2$. Therefore, the a-spinons condensate while spin-wave excitations are mapped by the b-spinons of the SBMFT. Applying the same procedure in the interaction (2), we get

$$V(t) = -\frac{\sqrt{2S}\sigma}{2} \gamma \hbar \sum_L [B_L^x(t) b_L^\dagger + \bar{B}_L^x(t) b_L], \quad (\text{B4})$$

where $B_L^x(t)$ are the spherical harmonic components of the oscillating magnetic field. In the interaction picture, the average of the operator $A(t)$ is expressed as $\langle A(t) \rangle = \langle S^\dagger(t) \hat{A}(t) S(t) \rangle$, where $S(t) = T_t \exp(-i \int \hat{V}(t') dt' / \hbar)$, and the caret denotes time evolution according to H_0 . It is a straightforward procedure to demonstrate that $S(t) = \exp[i\Phi + \sum_L \beta_L(t) b_L^\dagger - \bar{\beta}_L(t) b_L]$, where Φ is an irrelevant phase and the coherent eigenvalue, which is defined by $b|\beta\rangle = \beta|\beta\rangle$, is given by

$$\beta_L(t) = \sqrt{2\pi S \sigma \gamma B^x} \delta_{L0} \frac{e^{i(\gamma B^z - \omega_{\text{rf}} - i\eta)t}}{\gamma B^z - \omega_{\text{rf}} - i\eta}. \quad (\text{B5})$$

Here, we consider a monochromatic uniform magnetic field $B^x(t) = B^x e^{-i\omega_{\text{rf}}t}$, and η (the damping factor) is included for ensuring the convergence in the limit $t \rightarrow$

$-\infty$. The number of particles $N_i = |\beta_i|^2$ is then

$$N_i = \sum_{L'L} \frac{\bar{\beta}_{L'} \beta_L}{\sigma} \bar{Y}_{L'} Y_L = \frac{(\gamma B^x)^2 S}{2[(\gamma B^z - \omega_{\text{rf}})^2 + \eta^2]}, \quad (\text{B6})$$

which presents the maximum at the resonating condition $\gamma B^z = \omega_{\text{rf}}$. Following the same steps of Sec. (IV), we evaluate the magnetization dynamics on the spherical surface using the $U(1)$ coherent states of the HP formalism, which yields

$$\begin{aligned} M_i^\perp(t) &= \frac{\gamma \hbar}{\varepsilon^2} \langle S_i^+(t) \rangle = \frac{\gamma \hbar}{\varepsilon^2} \sqrt{\frac{2S}{\sigma}} \sum_L \beta_L(t) e^{-i\gamma B^z t} Y_L \\ &= \frac{M_s \gamma B^x(t)}{\gamma B^z - \omega_{\text{rf}} - i\eta}, \end{aligned} \quad (\text{B7})$$

which is identical to Eq. (32). The magnetic susceptibility is then determined from the above equation and we reach the same results obtained from the SBMFT.

-
- [1] S. Wolf, D. Awschalom, R. Buhrman, J. Daughton, S. Von Molnar, M. Roukes, A. Y. Chtchelkanova, and D. Treger, *Science* **294**, 1488 (2001).
- [2] I. Žutić, J. Fabian, and S. D. Sarma, *Reviews of Modern Physics* **76**, 323 (2004).
- [3] S. Zhang, *Physical Review Letters* **85**, 393 (2000).
- [4] J. Sinova, S. O. Valenzuela, J. Wunderlich, C. H. Back, and T. Jungwirth, *Reviews of Modern Physics* **87**, 1213 (2015).
- [5] K. Uchida, S. Takahashi, K. Harii, J. Ieda, W. Koshibae, K. Ando, S. Maekawa, and E. Saitoh, *Nature* **455**, 778 (2008).
- [6] K. Uchida, J. Xiao, H. Adachi, J.-i. Ohe, S. Takahashi, J. Ieda, T. Ota, Y. Kajiwara, H. Umezawa, H. Kawai, *et al.*, *Nature Materials* **9**, 894 (2010).
- [7] Y. Xu, D. Awschalom, and J. Nitta, *Handbook of spintronics* (Springer, 2016).
- [8] Y. Tserkovnyak, A. Brataas, and G. E. W. Bauer, *Physical Review B* **66**, 224403 (2002).
- [9] A. Azevedo, L. Vilela Leao, R. Rodriguez-Suarez, A. Oliveira, and S. Rezende, *Journal of Applied Physics* **97**, 10C715 (2005).
- [10] Y. Kajiwara, K. Harii, S. Takahashi, J.-i. Ohe, K. Uchida, M. Mizuguchi, H. Umezawa, H. Kawai, K. Ando, K. Takanashi, *et al.*, *Nature* **464**, 262 (2010).
- [11] A. Azevedo, L. Vilela-Leão, R. Rodríguez-Suárez, A. L. Santos, and S. Rezende, *Physical Review B* **83**, 144402 (2011).
- [12] Y. Ohnuma, H. Adachi, E. Saitoh, and S. Maekawa, *Physical Review B* **89**, 174417 (2014).
- [13] E. Saitoh, M. Ueda, H. Miyajima, and G. Tatara, *Applied Physics Letters* **88**, 182509 (2006).
- [14] T. Kimura, Y. Otani, T. Sato, S. Takahashi, and S. Maekawa, *Physical Review Letters* **98**, 156601 (2007).
- [15] S. O. Valenzuela and M. Tinkham, *Nature* **442**, 176 (2006).
- [16] K. Shen, G. Vignale, and R. Raimondi, *Physical Review Letters* **112**, 096601 (2014).
- [17] M. D. Stiles and A. Zangwill, *Physical Review B* **66**, 014407 (2002).
- [18] Q. He, Z. Wu, and C. Huang, *Journal of nanoscience and nanotechnology* **12**, 2943 (2012).
- [19] J. Li, Y. Hu, Y. Hou, X. Shen, G. Xu, L. Dai, J. Zhou, Y. Liu, and K. Cai, *Nanoscale* **7**, 9004 (2015).
- [20] G. M. Ziarani, M. Malmir, N. Lashgari, and A. Badiei, *RSC Advances* **9**, 25094 (2019).
- [21] P. Hsu, R. Bhattacharya, H. Gleskova, M. Huang, Z. Xi, Z. Suo, S. Wagner, and J. Sturm, *Applied physics letters* **81**, 1723 (2002).
- [22] P. Hsu, M. Huang, Z. Xi, S. Wagner, Z. Suo, and J. Sturm, *Journal of applied physics* **95**, 705 (2004).
- [23] V. Kotsubo and G. A. Williams, *Physical Review Letters* **53**, 691 (1984).
- [24] B. A. Ovrut and S. Thomas, *Physical Review D* **43**, 1314 (1991).
- [25] A. Moura, *Journal of Magnetism and Magnetic Materials* **513**, 167254 (2020).
- [26] S. J. Bereta, L. Madeira, V. S. Bagnato, and M. A. Caracanhas, *American Journal of Physics* **87**, 924 (2019).
- [27] A. Tononi and L. Salasnich, *Physical Review Letters* **123**, 160403 (2019).
- [28] Y. Colombe, E. Knyazchyan, O. Morizot, B. Mercier, V. Lorent, and H. Perrin, *EPL (Europhysics Letters)* **67**, 593 (2004).
- [29] M. White, H. Gao, M. Pasienski, and B. DeMarco, *Physical Review A* **74**, 023616 (2006).
- [30] T. van Zoest, N. Gaaloul, Y. Singh, H. Ahlers, W. Herr, S. Seidel, W. Ertmer, E. Rasel, M. Eckart, E. Kajari, *et al.*, *Science* **328**, 1540 (2010).
- [31] G. Condon, M. Rabault, B. Barrett, L. Chichet, R. Arguel, H. Eneriz-Imaz, D. Naik, A. Bertoldi, B. Battelier, P. Bouyer, *et al.*, *Physical Review Letters* **123**, 240402 (2019).
- [32] N. Lundblad, R. Carollo, C. Lannert, M. Gold, X. Jiang, D. Paseltiner, N. Sergay, and D. Aveline, *npj Microgravity* **5**, 1 (2019).

- [33] V. P. Kravchuk, D. D. Sheka, R. Streubel, D. Makarov, O. G. Schmidt, and Y. Gaididei, *Physical Review B* **85**, 144433 (2012).
- [34] V. P. Kravchuk, U. K. Rößler, O. M. Volkov, D. D. Sheka, J. van den Brink, D. Makarov, H. Fuchs, H. Fangohr, and Y. Gaididei, *Physical Review B* **94**, 144402 (2016).
- [35] D. D. Sheka, V. P. Kravchuk, and Y. Gaididei, *Journal of Physics A: Mathematical and Theoretical* **48**, 125202 (2015).
- [36] Y. Gaididei, V. P. Kravchuk, and D. D. Sheka, *Physical review letters* **112**, 257203 (2014).
- [37] R. Streubel, P. Fischer, F. Kronast, V. P. Kravchuk, D. D. Sheka, Y. Gaididei, O. G. Schmidt, and D. Makarov, *Journal of Physics D: Applied Physics* **49**, 363001 (2016).
- [38] A. Trumper, L. Manuel, C. Gazza, and H. Ceccatto, *Physical review letters* **78**, 2216 (1997).
- [39] M. Gonzalez, E. A. Ghioldi, C. J. Gazza, L. O. Manuel, and A. E. Trumper, *Physical Review B* **96**, 174423 (2017).
- [40] E. A. Ghioldi, M. G. Gonzalez, S.-S. Zhang, Y. Kamiya, L. O. Manuel, A. E. Trumper, and C. D. Batista, *Physical Review B* **98**, 184403 (2018).
- [41] S.-S. Zhang, E. Ghioldi, Y. Kamiya, L. Manuel, A. Trumper, and C. Batista, *Physical Review B* **100**, 104431 (2019).
- [42] T. N. De Silva, M. Ma, and F. C. Zhang, *Physical Review B* **66**, 104417 (2002).
- [43] D. P. Hardin, T. Michaels, and E. B. Saff, *Dolomites Research Notes on Approximation* **9** (2016).
- [44] N. Teanby, *Computers & Geosciences* **32**, 1442 (2006).
- [45] C. J. De Leone and G. T. Zimanyi, *Physical Review B* **49**, 1131 (1994).
- [46] T. Holstein and H. Primakoff, *Physical Review* **58**, 1098 (1940).
- [47] D. P. Arovas and A. Auerbach, *Physical Review B* **38**, 316 (1988).
- [48] S. Sarker, C. Jayaprakash, H. R. Krishnamurthy, and M. Ma, *Physical Review B* **40**, 5028 (1989).
- [49] A. Auerbach, *Interacting electrons and quantum magnetism* (Springer Science & Business Media, 2012).
- [50] W.-M. Zhang, R. Gilmore, *et al.*, *Reviews of Modern Physics* **62**, 867 (1990).
- [51] A. Perelomov, *Generalized coherent states and their applications* (Springer Science & Business Media, 2012).
- [52] R. J. Glauber, *Physical Review* **131**, 2766 (1963).
- [53] Y. Shiomi and E. Saitoh, *Physical Review Letters* **113**, 266602 (2014).
- [54] P. Mesquita and A. Moura, *Journal of Physics: Condensed Matter* **32**, 305802 (2020).
- [55] C. Itoi and M. Kato, *Journal of Physics A: Mathematical and General* **27**, 2915 (1994).